ELSEVIER

Scopus

doi

Journal of Vibration Engineering

ISSN:1004-4523

Registered

- SCOPUS
- GOOGLE SCHOLAR
- DIGITAL OBJECT IDENTIFIER (DOI)
- IMPACT FACTOR 6.1

Our Website
www.jove.science

Double Dispersive Chemically Reactive Flow in an Inclined Porous Channel with Dufour Effect, Viscous Dissipation, and Slip Boundary Conditions

Jagadeeshwar Pashikanti [1], Vengala Narender [2*], Susmitha Priyadharshini D R [3]

[1]Department of Science and Humanities, Indian Institute of Information Technology Tiruchirappalli, Tamil Nadu, 620012, India

[2]Department of Mathematics, Vardhaman College of Engineering Hyderabad, Telangana, 501218, India

[3]Department of Mathematics, National Institute of Technology Andhra Pradesh, Tadepalligudem, Andhra Pradesh, India

Abstract

The present work investigates heat and mass transfer characteristics in an inclined porous channel by incorporating the effects of double dispersion, Dufour diffusion, chemical reaction, and viscous dissipation under slip boundary conditions. Thermal and solutal dispersion mechanisms are considered to accurately model transport phenomena in porous media. A first-order homogeneous chemical reaction is assumed, while viscous dissipation is included to account for internal heat generation. The system of nonlinear equations governing momentum, energy, and concentration is transformed into a coupled system of ordinary differential equations using suitable similarity transformations and are solved numerically using the Successive Quadratic Linearization Method (SQLM). In addition, an entropy generation analysis is performed to assess thermodynamic irreversibility arising from heat transfer, fluid friction, and mass diffusion. The influences of key parameters such as slip parameter, dispersion coefficients, Dufour number, chemical reaction parameter, inclination angle, Brinkman number, and Eckert number on entropy generation rate, velocity, temperature, concentration, and Bejan number are examined. The results indicate that enhanced Dufour and viscous dissipation effects significantly increase temperature and entropy generation, whereas stronger chemical reactions suppress concentration and reduce solutal irreversibility. The present findings are relevant to the optimization of thermal systems involving porous channels and reactive transport processes.

Keywords: Buongiorno model, Double dispersion, Chemical reaction, Dufour effect, Viscous dissipation, Porus medium, Entropy generation, Graphene nanofluids

1. Introduction

Nano fluids are favored over traditional viscous micro fluids due to their superior heat transfer capabilities. Moreover, they help to keep the flow channels clear of blockages, deposits, and wear. It has been reported that the principal contributors to slip phenomena in nanofluid flows are thermophoresis and Brownian diffusion [1]. The effectiveness of nano fluids depends on factors such as geometry selection, base fluids, volume fraction, hybrid nanoparticles, and specific application requirements.[3]. Nevertheless, findings from computational analyses reveal that Graphene oxide (GO) is known to markedly improve heat transfer owing to its excellent thermal conductivity [5, 6, 7, 8]. Graphene–based nanofluids have diverse applications, including lithium–ion batteries, biosensing devices, supercapacitors, and biomedical suspensions.

Several foundational numerical investigations have examined fluid flow in inclined channels have systematically explored fully developed laminar flow between two parallel plates set at an angle. Counterflow conditions were examined under uniform flux with characteristics of actual flow [9]. Both theoretical and experimental studies report

that, among graphene-based nanofluids, graphene oxide (GO) and hybrid graphene nanoparticles dispersed in ethylene glycol and water have been extensively explored, due to their favourable thermophysical properties. Analytical studies concerning the flow of GO nanofluids in channels bounded by an increase in nanoparticle volume fraction results in enhanced heat transfer performance when the plates are in motion [20]. The combination of graphene- based nanofluids with metallic or semiconductor nanoparticles and polymeric materials significantly enhances their industrial applicability. These hybrid nanofluids are utilized in adsorptive technologies, lubrication enhancement, humidity sensors, photocatalytic reactions, and advanced heat-transfer systems. [5]. The magnetohydrodynamic (MHD) behaviour of water–graphene oxide (W–GO) nanofluids flowing through a horizontal channel under the action of forced convection has been examined. Integrating magnetohydrodynamic studies with nanofluid behaviors is crucial for industrial and biomedical applications, such as molten pumps used for coolant circulation in nuclear reactors and applications in modern drug delivery systems. Likewise, investigations into the impact of viscous dissipation on flow behavior enhances our understanding of energy losses resulting from fluid particle interactions, which can improve the use of fluids as efficient lubricants [13]. In this regard, the transport of two micropolar fluids driven by a uniform pressure gradient through distinct porous layers with different thermophysical properties was investigated. Computational fluid dynamics research under convective conditions, Entropy characteristics in an inclined channel transporting a micropolar fluid under convective and slip boundary conditions were also analyzed, and the findings revealed that both the Reynolds number and the coupling parameter play a dominant role in regulating entropy generation [15].

Fluid flow along with coupled heat–mass transfer phenomena in inclined porous channels is an active area of research of considerable importance due to their applications in chemical reactors, geothermal energy systems, porous heat exchangers, and thermal management devices. In many microscale and rarefied flow situations, the classical no-slip boundary assumption is no longer valid, and therefore slip boundary conditions must be employed to accurately describe the fluid behavior near solid surfaces [55]. The presence of a porous medium significantly alters momentum, thermal, and solutal transport characteristics, particularly when the flow is influenced by channel inclination. To realistically capture transport mechanisms in porous structures, the inclusion of double dispersion, accounting for both thermal and solutal dispersion effects, is essential. Recent studies have emphasized the importance of cross-diffusion phenomena such as the Dufour effect, which represents heat flux induced by concentration gradients and plays a key role in coupled thermo-solutal transport processes [50, 54]. Furthermore, the inclusion of chemical reaction effects is crucial for modeling industrial and environmental processes, while viscous dissipation contributes to internal heat generation in flows with high velocity gradients [56]. Although several investigations have addressed individual or combined effects of slip, dispersion, and cross-diffusion in porous media flows, studies that simultaneously consider double dispersion, Dufour diffusion, chemical reaction are still lacking.

Additionally, Graphene exhibits exceptionally high thermal conductivity compared with most known materials. Owing to its advantageous thermophysical, mechanical, and chemical properties, its use as a coolant has gained increasing attention. Its significance in renewable energy promotes cost-effective practical large-scale applications in power storage and capacity expansion. This importance highlights the need for computational research on graphene-based nanofluid flows in various geometries. The objective of this study was to address the gap in the computational analysis of the research models the transport of graphene oxide nanoparticles in water through an inclined channel, employing numerical techniques to solve the governing equations and interpret the flow behavior.

2. Mathematical formulation

The physical setup comprises two parallel plates inclined at an angle α, between which a steady flow of water-based graphene oxide (GO) nanofluid is sustained. The schematic illustration of the flow domain is presented in figure 1.

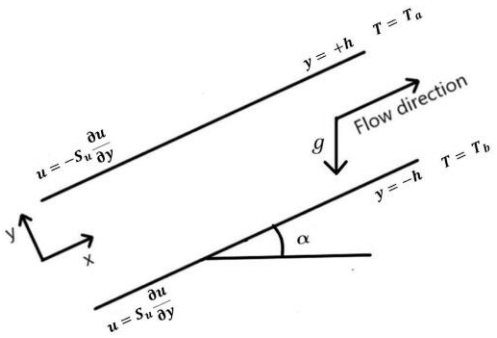

Figure 1: Schematic representation of the probl

In this study, the flow formulation incorporates the influence of gravitational body forces along with key nanoparticle transport mechanisms, specifically Brownian diffusion and thermophoretic effects. Accordingly, the governing equations are developed using the Buongiorno nanofluid framework [1], leading to the following mathematical model:

$$\frac{\partial u}{\partial x} = 0 \qquad (1)$$

$$\rho_{nf}\left(v_0 \frac{\partial u}{\partial y}\right) + \frac{\partial p}{\partial x} = \mu_{nf}\frac{\partial^2 u}{\partial y^2} + [(\rho\beta)_{nf}(T - T_a)(1 - C_a) - (\rho_{sp} - \rho_{bf})(C - C_a)]gsin\ \alpha - \frac{\mu_{nf}}{\kappa_p}u - \sigma_{nf}B_0^2 u \qquad (2)$$

$$\frac{\partial}{\partial y}\left(\alpha_e \frac{\partial T}{\partial y}\right) + \frac{D_B k_T \rho_{nf}}{(\rho C_p)_{nf} C_s}\frac{\partial^2 C}{\partial y^2} + \frac{\mu_{nf}}{(\rho C_p)_{nf}}\left(\frac{\partial u}{\partial y}\right)^2 = 0 \qquad (3)$$

$$\frac{\partial}{\partial y}\left(D_e \frac{\partial C}{\partial y}\right) + \frac{D_T}{T_a}\frac{\partial^2 T}{\partial y^2} + K_c(C - C_a) = 0 \qquad (4)$$

The slip boundary conditions corresponding to this configuration are expressed as

$$y = -h : u = S_u \frac{\partial u}{\partial y}, T = T_a, C = C_a \qquad (5)$$

$$y = h : u = -S_u \frac{\partial u}{\partial y}, T = T_b, C = C_b \qquad (6)$$

The symbols T_b and T_a are the fluid temperatures at the lower plate and upper plate respectively and Similarly, C_b and C_a denote the nanofluid concentrations at the lower and upper plates, respectively. The parameter U_0 represents the reference velocity, while h, k_m, κ, and D_m refer to the heat transfer coefficients at the channel plates, the mass transfer coefficient, the thermal conductivity, and the mass diffusivity of the nanofluid. Also, $\alpha_e = \alpha_{nf} + \gamma du$ and $D_e = D_B + \omega du$ are respectively the effective thermal and solutal diffusivities and γ and ω are the coefficients of thermal and solutal dispersions.

$$\mu_{nf} = \frac{\mu_{bf}}{(1-\Phi)^{2.5}}$$
$$\rho_{nf} = (1-\Phi)\rho_{bf} + \Phi\rho_{sp}$$
$$\alpha_{nf} = \frac{\kappa_{nf}}{(\rho C_p)_{nf}}$$
$$(\rho C_p)_{nf} = (1-\Phi)(\rho C_p)_{bf} + \Phi(\rho C_p)_{sp}$$
$$(\rho\beta)_{nf} = (1-\Phi)(\rho\beta)_{bf} + \Phi(\rho\beta)_{sp}$$
$$\frac{\kappa_{nf}}{\kappa_{bf}} = \frac{\kappa_{sp} + 2\kappa_{bf} + 2\Phi(\kappa_{bf} - \kappa_{sp})}{\kappa_{sp} + 2\kappa_{bf} - \Phi(\kappa_{bf} - \kappa_{sp})}$$
$$\frac{\sigma_{nf}}{\sigma_{bf}} = \frac{\sigma_{sp} + 2\sigma_{bf} + 2\Phi(\sigma_{bf} - \sigma_{sp})}{\sigma_{sp} + 2\sigma_{bf} - \Phi(\sigma_{bf} - \sigma_{sp})}$$

The subscripts *nf*, *bf*, and *sp* correspond to the nanofluid, base fluid, and solid particles respectively. The symbols

Table 1: Values of thermophysical properties [19, 20, 21, 22]

Property (Units)	Water	Graphene oxide
ρ (kg/m^3)	997.1	1800
C_p (J/kgK)	4179	717
κ (W/mK)	0.613	5000
β $(10^{-5}/K)$	21	28.4
σ (S/m)	0.005	10^7

κ, C_p, β, ρ, μ, and σ represent thermal conductivity, the specific heat capacity, thermal expansion coefficient, density, dynamic viscosity, and electrical conductivity. The governing equations 1–4 are transformed using the following similarity variables:

$$\eta = \frac{y}{h}, u = U_0 f(\eta), \theta(\eta) = \frac{T - T_a}{T_b - T_a}, \phi(\eta) = \frac{C - C_a}{C_b - C_a} \qquad (7)$$

The transformed ordinary differential equations (ODEs) along with their boundary conditions are expressed as

$$f'' - A_1 R_{SC} f' + \frac{Gr}{Re} A_2 (A_3\theta - N_r\phi) sin\ \alpha - \frac{f}{D_a} - A_4 Ha\, f - A_2 P_1 = 0 \qquad (8)$$
$$A_5 P_r D_h (f'\theta' + f\theta'') + \theta'' + D_u P_r A_\alpha \phi'' + A_6 E_c P_r (f')^2 = 0 \qquad (9)$$
$$D_c S_c (f'\phi' + f\phi'') + \phi'' + \frac{N_t}{N_b}\theta'' + C_R S_c \phi = 0 \qquad (10)$$

such that

$$\eta = -1 : f - S f' = 0, \theta = 0, \varphi = 0 \qquad (11)$$
$$\eta = 1 : f + S f' = 0, \theta = 1, \varphi = 1 \qquad (12)$$

The constant coefficients (A_i, $i = 1, \ldots, 6$) and the nondimensional parameters used in the formulation namely, the suction/injection parameter R_{SC}, buoyancy ratio N_r, slip parameter, heat capacity ratio τ, Brownian motion parameter N_b, thermophoresis parameter N_t, Gasthof number Gr, and Reynolds number Re are defined as

$$
\begin{aligned}
&A_1 = \left(1 - \Phi + \Phi\frac{\rho_{sp}}{\rho_{bf}}\right), A_2 = (1-\Phi)^{2.5}, A_3 = 1 - \Phi + \Phi\frac{(\rho\beta)_{sp}}{(\rho\beta)_{bf}},\\
&A_4 = \frac{\sigma_{nf}}{\sigma_{bf}}(1-\Phi)^{2.5}, A_5 = \left(1 - \Phi + \Phi\frac{(\rho C_p)_{sp}}{(\rho C_p)_{bf}}\right),\\
&A_6 = \left(1 - \Phi + \Phi\frac{(\rho C_p)_{sp}}{(\rho C_p)_{bf}}\right)\frac{\kappa_{bf}}{\kappa_{nf}},\\
&S = \frac{S_u}{h}, R_{sc} = \frac{\rho_{bf}\nu_0 h}{\mu_{bf}},\\
&Gr = \frac{g\beta_{bf}(T_b - T_a)(1-C_a)h^3\rho_{bf}^2}{\mu_{bf}^2}, P_1 = \frac{h^2}{U_0\mu_{nf}}\frac{\partial p}{\partial x},\\
&N_r = \frac{(\rho_{sp} - \rho_{bf})(C_b - C_a)}{(\rho\beta)_{bf}(1-C_a)(T_b - T_a)},\\
&Re = \frac{\rho_{bf}U_0 h}{\mu_{bf}}, N_b = \frac{\tau D_B(C_b - C_a)}{\alpha_{nf}}, N_t = \frac{\tau D_T(T_b - T_a)}{\alpha_{nf}T_a},\\
&D_h = \frac{\gamma d U_0}{\mu_{bf}}, D_u = \frac{D_B k_T \rho_{bf}(C_b - C_a)}{C_{pbf}C_s(T_b - T_a)},\\
&S_r = \frac{D_T k_T (T_b - T_a)}{D_B T_a (C_b - C_a)}, Pr = \frac{\mu_{bf}C_{pbf}}{k_{bf}},\\
&Ha = \frac{\sigma_{bf}B_0^2 h^2}{\mu_{bf}}, D_s = \frac{\omega d U_0}{\mu_{bf}}
\end{aligned}
\tag{13}
$$

The key quantities of practical interest, namely the Nusselt number Nu, Sherwood number Sh, and skin friction coefficient C_f, are derived as

$$Nu = -\theta'(\eta), Sh = -\phi'(\eta), Re\ C_f = A_7 f'(\eta), \text{at } \eta = \pm 1 \tag{14}$$

Here, $A_7 = (1-\Phi)^{-2.5}\left[(1-\Phi) + \Phi\left(\frac{\rho_{sp}}{\rho_{bf}}\right)\right]^{-1}$ is a constant. In the following section, an analysis of entropy generation is presented, and the corresponding entropy generation number is derived.

3. Entropy Analysis

Entropy generation analysis is conducted to quantify and minimize energy losses, thereby enhancing the efficiency of the model and overall system performance. In accordance with the second law of thermodynamics, entropy is produced due to temperature gradients, viscous dissipation, and concentration differences. Accordingly, the dimensional entropy generation rate S_G can be expressed as [23]:

$$S_G = \frac{\kappa_{nf}}{T_a^2}\left(\frac{\partial T}{\partial y}\right)^2 + \frac{\mu_{nf}}{T_a}\left(\frac{\partial u}{\partial y}\right)^2 + RD_B\left[\frac{1}{C_a}\left(\frac{\partial C}{\partial y}\right)^2 + \frac{1}{T_a}\left(\frac{\partial T}{\partial y}\right)\left(\frac{\partial C}{\partial y}\right)\right] \tag{15}$$

Here, the terms on the right-hand side correspond to thermodynamic irreversibilities due to temperature gradients, fluid friction, and coupled heat–mass transfer effects. Using the dimensional entropy generation rate S_G and the characteristic entropy scale

$$S_{G0} = \frac{\kappa_{nf}(T_b - T_a)^2}{(T_a L)^2} \quad ,$$

the nondimensional entropy generation number is defined as

$$N_S = \frac{S_G}{S_{G0}}$$

From equation (27), we have

$$\frac{\eta^2}{4} N_S = \frac{1}{\chi}\left[\theta'^2 + A_6 \frac{Ec\, Pr}{\Omega_T}\, f'^2 + A_5 M_m \frac{\Omega_C}{\Omega_T}\, \phi' \left(\frac{\Omega_C}{\Omega_T}\phi' + \theta'\right)\right]$$

$$= N_{S_h} + N_{S_G} \qquad (16)$$

Here, the subscripts S_h and S_G denote the irreversibilities associated with heat transfer and those arising from fluid friction along with coupled heat–mass transfer, respectively. The parameters appearing in (16) are defined as follows: the geometric parameter $\chi = h^2/L^2$, the temperature ratio $\Omega_T = T_b/T_a$, the concentration ratio $\Omega_C = C_b/C_a$, and the combined heat–mass transfer parameter

$$M_m = \frac{R\, D_B\, C_a}{\kappa_{bf}}$$

The Eckert number is given by

$$E_c = \frac{U_0^2}{\kappa_{bf}\, C_{pbf}\, (T_b - T_a)}$$

the Prandtl number as

$$Pr = \frac{\mu_{bf}\, C_{pbf}}{\kappa_{bf}}$$

and the constant

$$A_6 = (1 - \Phi)^{-2.5} \frac{\kappa_{bf}}{\kappa_{nf}}$$

The Bejan number, representing the ratio of heat transfer irreversibility to total entropy generation, is defined as $Be = \frac{N_{Sh}}{N_S}$, is used to identify the dominant mechanism responsible for entropy generation [23]. Based on this ratio, heat transfer is the primary contributor when $Be > 0.5$, whereas fluid friction together with coupled heat–mass transfer dominates when $Be < 0.5$. For $Be = 0.5$, all three sources of irreversibility contribute equally to the total entropy generation [25]

4. Numerical Solution

The spectral quasilinearization method, as proposed by Bellman and Canuto [26, 27], is employed to solve the system of transformed ordinary differential equations. Initially, the spectral collocation method is applied to linearize the coupled nonlinear equations. Using Chebyshev polynomials to approximate the functions at the Gauss–Lobatto collocation points, a matrix equation is formed. The resulting equation is then solved iteratively, starting from initial approximations that satisfy the boundary conditions.

5. Results

In this section, the results are illustrated graphically and discussed in detail. The governing parameters are systematically varied within practical limits to assess their effects. as suggested in the literature [28]. Since the water-based nanofluid exhibits Newtonian behaviour, fixed values of the nanoparticle volume fraction and Prandtl number are considered as $\Phi = 0.01$ and $Pr = 6.5$, respectively. Unless stated otherwise, the remaining parameter values are selected as $Ec = 10^{-5}$, $S = 0.5$, $R_{SC} = 5$,$Re = 300$, $\alpha = \pi/4$,$N_r = 2$,$Gr = 2 \times 10^5$, $N_b = 4 \times 10^{-4}$, and $N_t = 2 \times 10^{-4}$. The SQLM approximation is implemented with order $N = 100$, and the solution converges by the tenth iteration.

Figure (2) shows that as chemical reaction increases, a drop in fluid velocity.

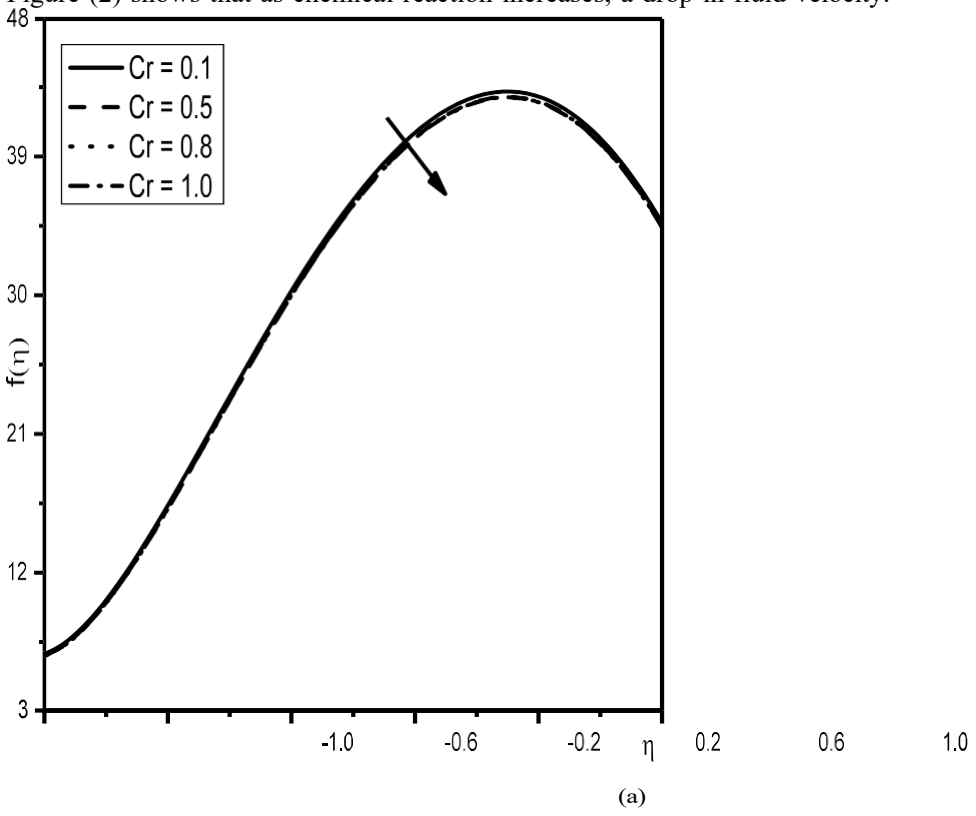

(a)

Figure 2: Influence of C_r on f

Figure (3) explores the strength of Re on f , θ, φ, Be, and N_S. As the Re , enhances, results in reduction of viscous forces, which results in diminish flow and hence there is go down in flow velocity (figure (3a)). Similarly, the reduced viscous forces decrease the nanofluid temperature as shown in the figure (3b), the concentrated fluid moves with lesser velocity causing a drop in convective mass transfer. Thus, the concentration of the nanofluid increases (figure (3c)). In the same way, entropy number decreases , when Re is varied as shown in the figure (3d). This leads to an increase in the Bejan number Be, indicating a greater contribution of fluid friction and mass transfer to the total entropy generation, as illustrated in Figure (3e).

Figure (4) narrates the strengths of R_{SC} on velocity f , θ, φ, entropy number N_S and Bejan number Be. As the values of R_{SC} escalates, the fluid flow f decreased in the proximity of the cooler plate. Whereas, in the middle of the channel, as expected, fluid suction, causes thinning of the boundary layer and reduces the velocity, as shown in the figure (4a). As suction/injection parameter increases the temperature decreases and concentration increases as

shown in figures (4b), (4c). Figure (4d) showcases the increases in entropy number between $-1 < \eta < -0.37$ and $0.22 < \eta < 0.86$, whereas, it depicts a decrease in $-0.37 < \eta < 0.22$ and $0.86 < \eta < 1$. Even though the Bejan number *Be* increases as seen in the figure (4e), showcasing the allowance of mass transfer as well as fluid friction irreversibility contributes to the increased entropy throughout the channel.

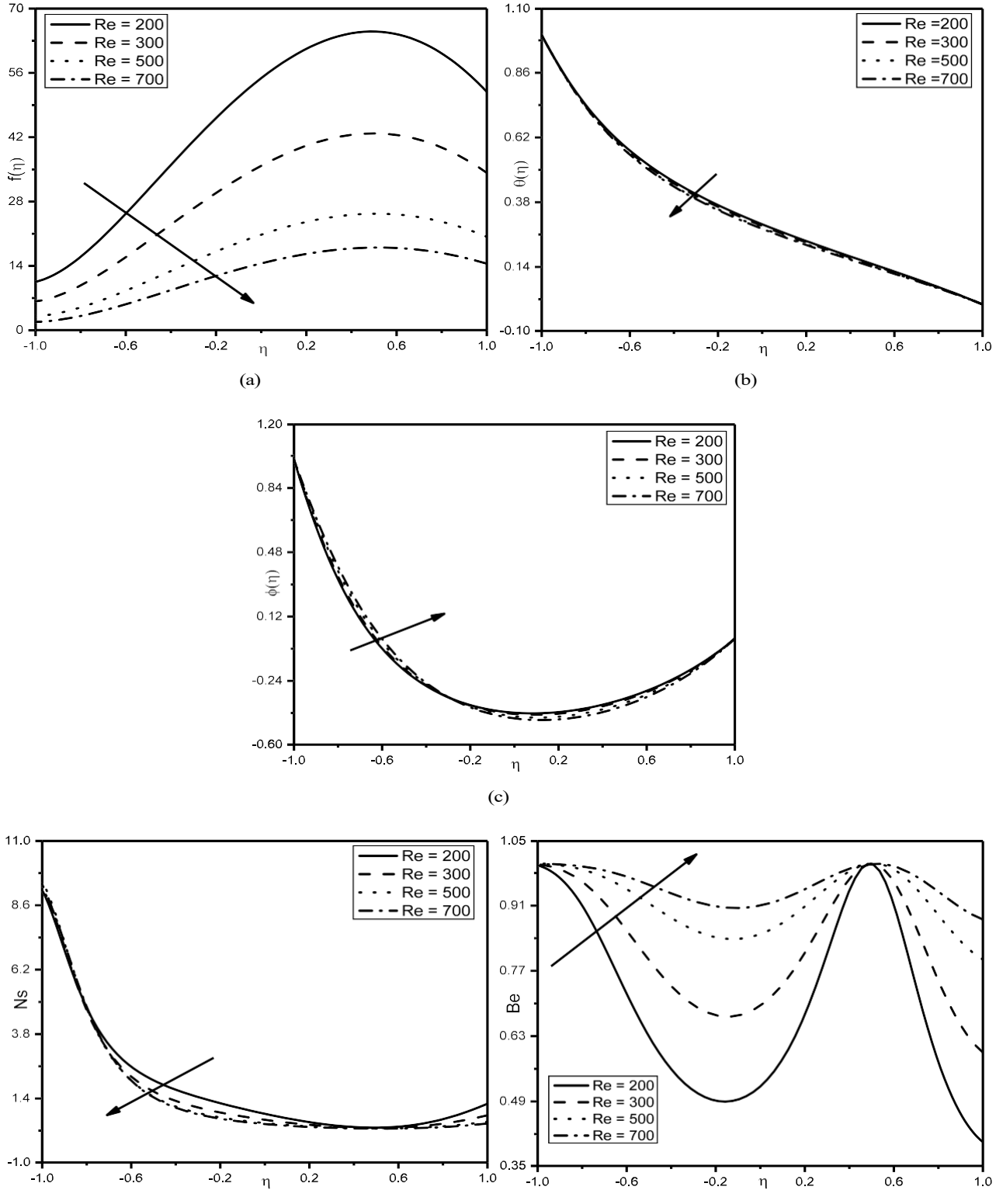

Figure 3: Influence of Re on (a) f, (b) θ, (c) φ, (d) N_S and (e) Be

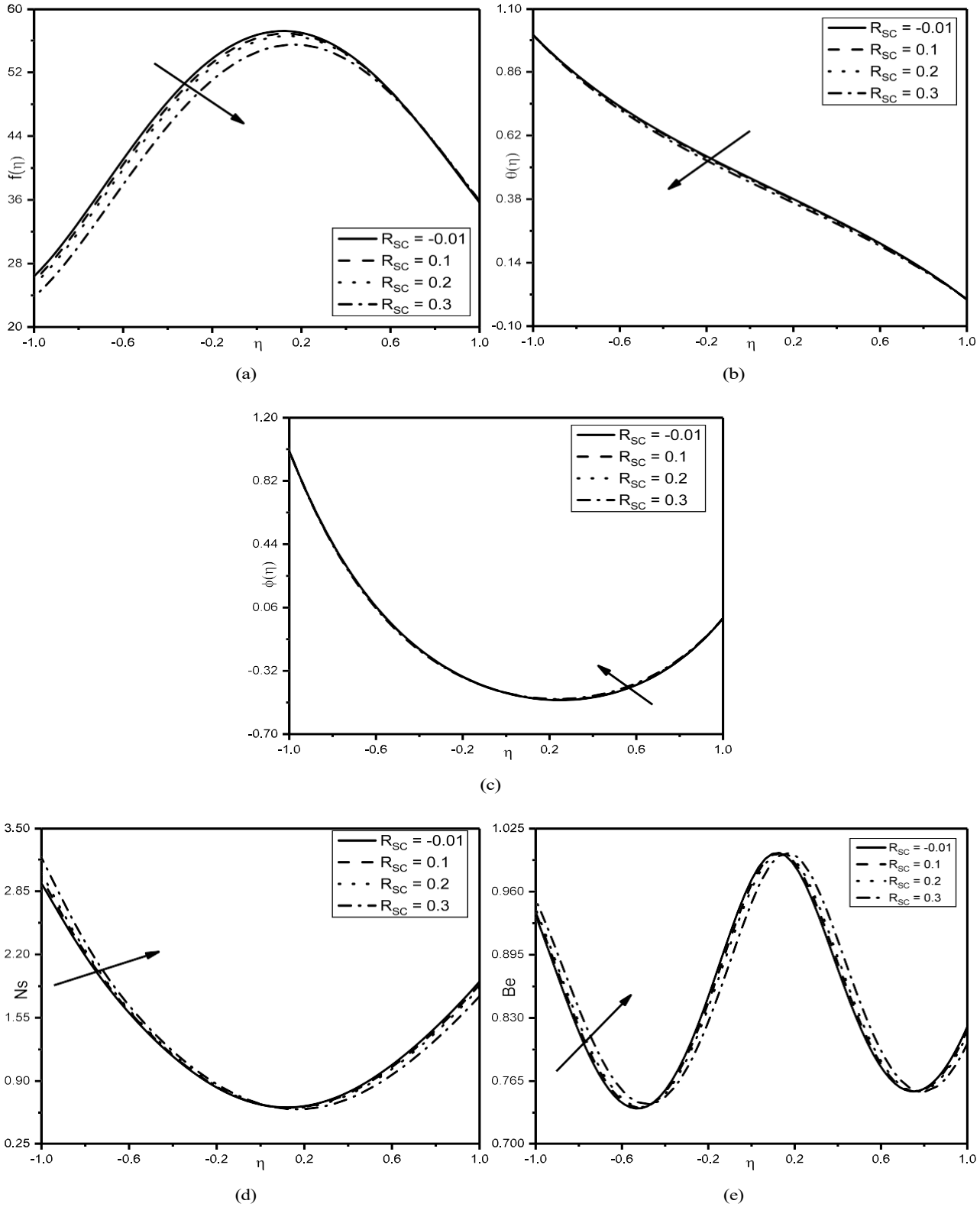

Figure 4: Influence of R_{SC} on (a) f, (b) θ, (c) φ, (d) N_S and (e) Be

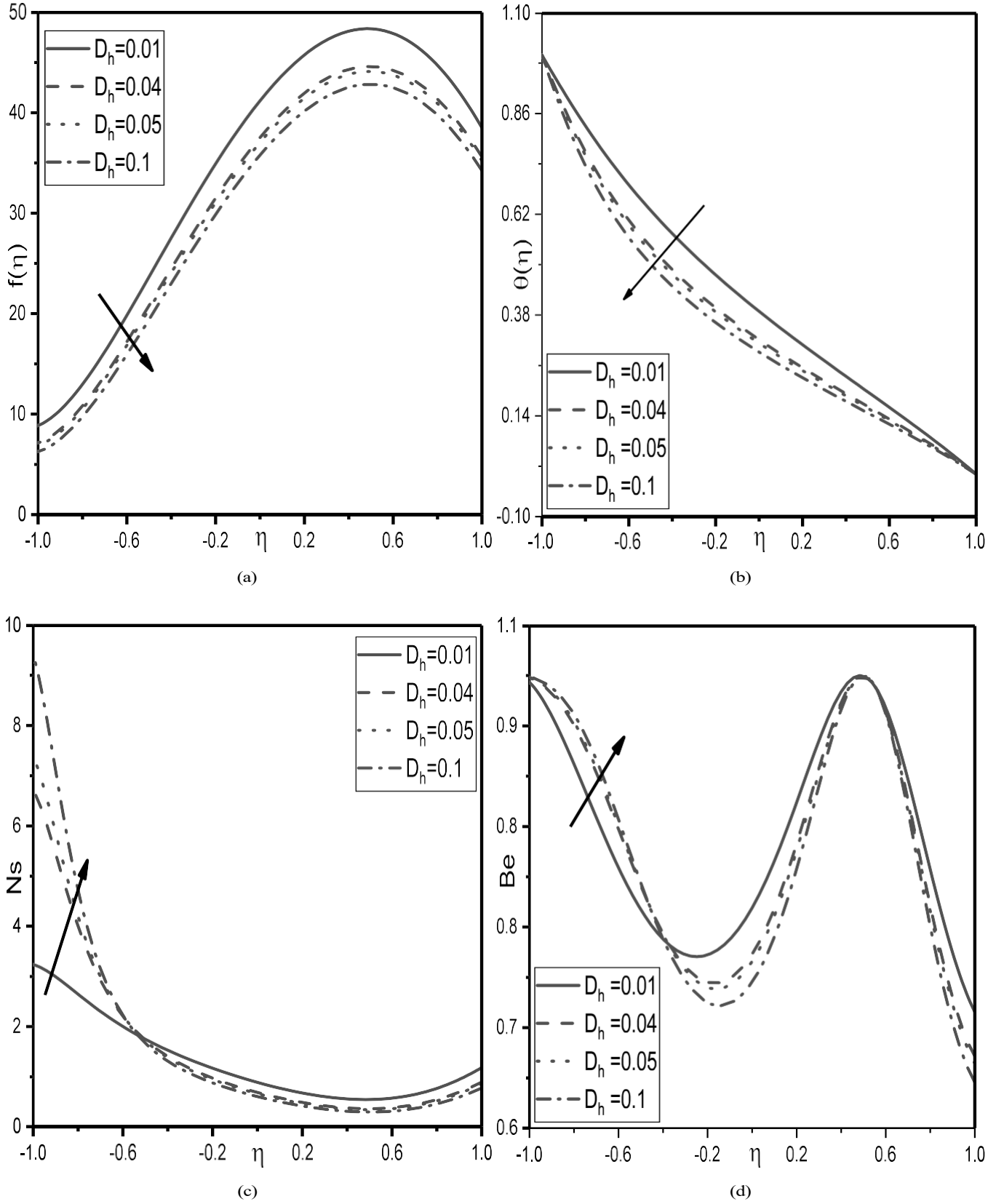

Figure 5: Influence of *Dh* on (a) f, (b) θ, (c) N_S and (d) *Be*

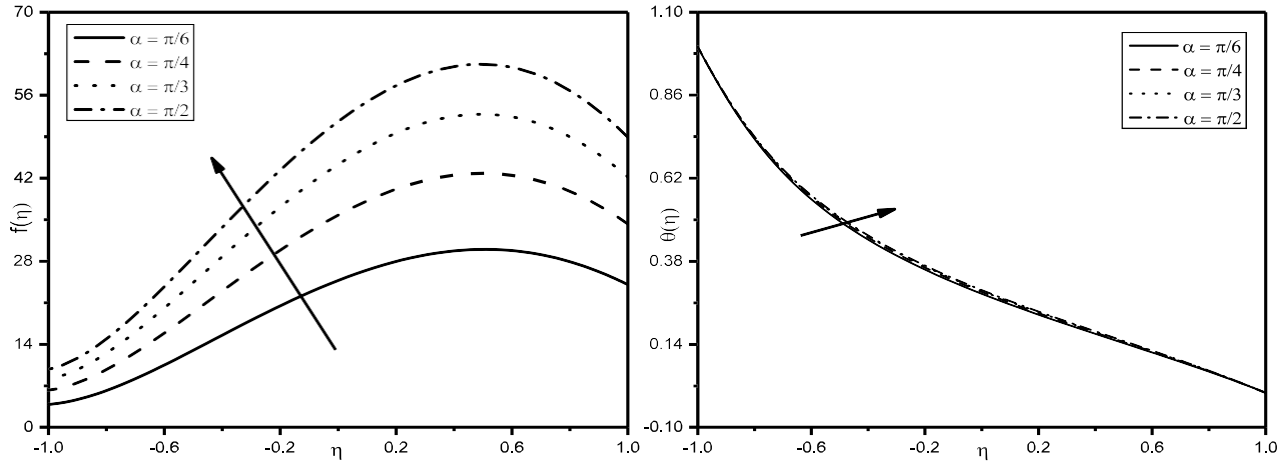

(a) (b)

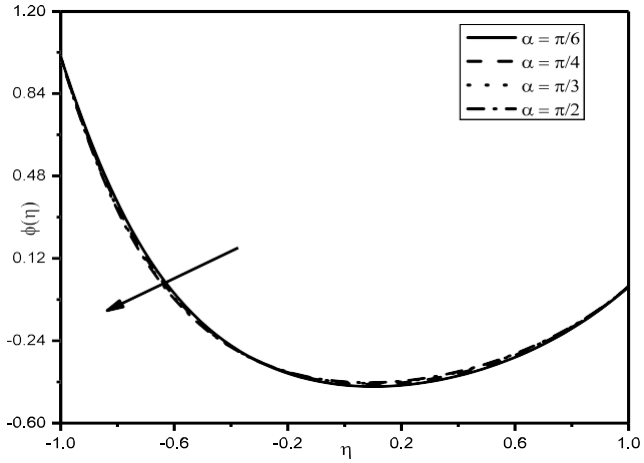

(c)

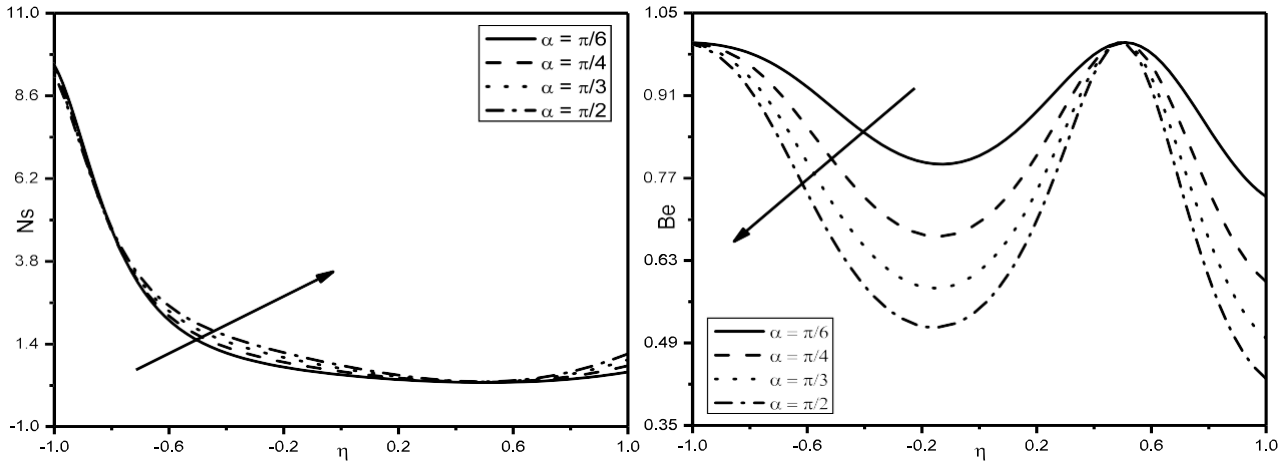

(d) (e)

Figure 6: Influence of α on (a) f, (b) θ, (c) φ, (d) N_S and (e) Be

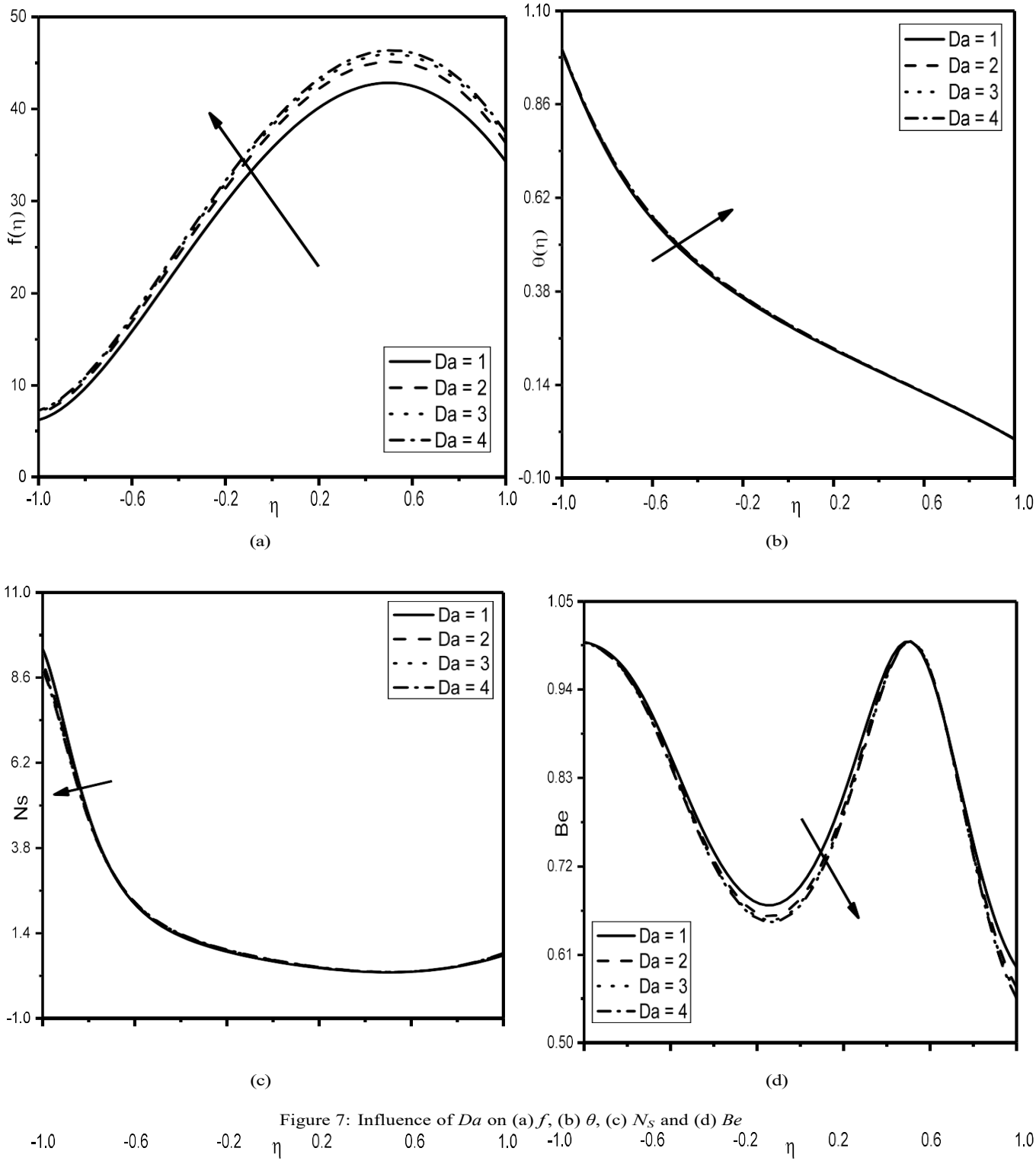

Figure 7: Influence of Da on (a) f, (b) θ, (c) N_S and (d) Be

Figure (5) demonstrates influence of Dh on the strengths of f, θ, N_S and Be. Escalating the value of thermal dispersion parameter Dh, fluid velocity decreases (5a) and temperature decreases (5b), thus increasing the entropy generation and hence N_S increases as shown in the figure (5c). Whereas, it impacts in enhancement of Bejan number Be (figure (5d)). Hence, thermal dispersion parameter mildly contributes to generation of entropy from combined mass and heat transfer together with fluid friction, even though the overall $Be > 0.5$, and the energy dissipation is

pronounced from heat transfer.

Figure (6) illustrates the influence of the inclination angle α on f, θ, φ, N_S, and Be. As the increase in angle of inclination occurs, enlargement in velocity is observed, due to the impacts of gravitational force (figure (6a)). Similarly, the nanofluid temperature increases with α values as shown in the figure (6b).In contrast, a slight decrease in concentration is observed with increasing α, as depicted in Figure (6c). Likewise, as α increase, resulting in increment of N_S values as shown in the figure (6d) implying reduction in the Bejan number Be to decrease (figure (**??**)), thus establishing the mild allowance of mass transfer in conjunction with fluid friction to the generated entropy, even though the overall entropy is generated from heat transfer, similar to the previous case.

Figure (7) examines the effect of the Darcy number Da on fluid velocity, temperature, entropy generation number, and Bejan number. Figure (7a) illustrates that increasing Da increases fluid velocity. Similarly, from figure (7b), Da values indicate an increase in temperature, due to elevated thermal conductivity of graphene oxide nanofluid. In the same way, strengthening Da, a reduction in N_S is observed, since the dissipation is minimized and heat is transferred to the fluid due to high thermal conductivity (figure (7c)). This projects a depliation in Be (figure (7d)) which resounds the mild allowance of mass transfer in conjunction with fluid friction to the produced entropy.

Figure (8) demonstrates influence of Ds on the strengths of f, θ, φ, N_S and Be. Escalating the value of solutal dispersion parameter Ds, fluid velocity increases (figure (8a)) and temparature slitely increases due to collision of particles (figure (8b)). where as reduced concentration is observed (figure (8c)), thus decreasing the entropy generation and hence N_S decreases as shown in the figure (8d). Whereas, it impacts the enhancement of Bejan number Be (figure (8e)). Hence, solutal dispersion parameter contributes to generation of entropy from combined mass and heat transfer together with fluid friction, even though the overall $Be > 0.5$, and the energy dissipation is pronounced from heat transfer.

Figure (9) illustrates the influence of the Dufour number Du on the fluid velocity, temperature distribution, entropy generation number, and Bejan number. Figure (9a) shows that increasing Du increases fluid velocity. Similarly, from figure (9b), Du values indicate an increase in temperature, due to the duffer effect on nanofluid. In the same way, strengthening Du, a reduction in N_S is observed, (figure (9c)). This causes a reverse trend in Bejan number Be (figure (9d)) which resounds the mild allowance of mass transfer in conjunction with fluid friction contributing to the generated entropy.

Figure (10) explores the strength of Ec on f, N_S and Be. As the Ec , increases, an enhanced fluid folw is observed (figure (10a)). In the same way, entropy number increases, when Ec is varied as shown in the figure (10b). This leads to a reduction in the Bejan number Be, indicating an increased contribution of fluid friction and mass transfer irreversibilities to the total entropy generation, as illustrated in Figure (10c).

Figure (11) depicts the strength of S on f, θ, φ, N_S and Be. Figure (11a) shows that increasing the S value , fluid velociy increases.. Similarly, figure (11b) explores that as S enhances, resulting in increase in the heat transfer coefficient and hence the heated fluid flows with notable velocity. Thus, the nanofluid closer to the hotter lower plate flows with enhanced temperature (11b) and with reduced concentration (11c). Similarly, it is witnessed through the figure (11d) that as S strengthens, notable depliation in the coefficient of heat transfer takes place and hence the generation of entropy too. This causes an elevation of Be (figure (11e)), thus indicating the strength of irreversibility of heat transfer.

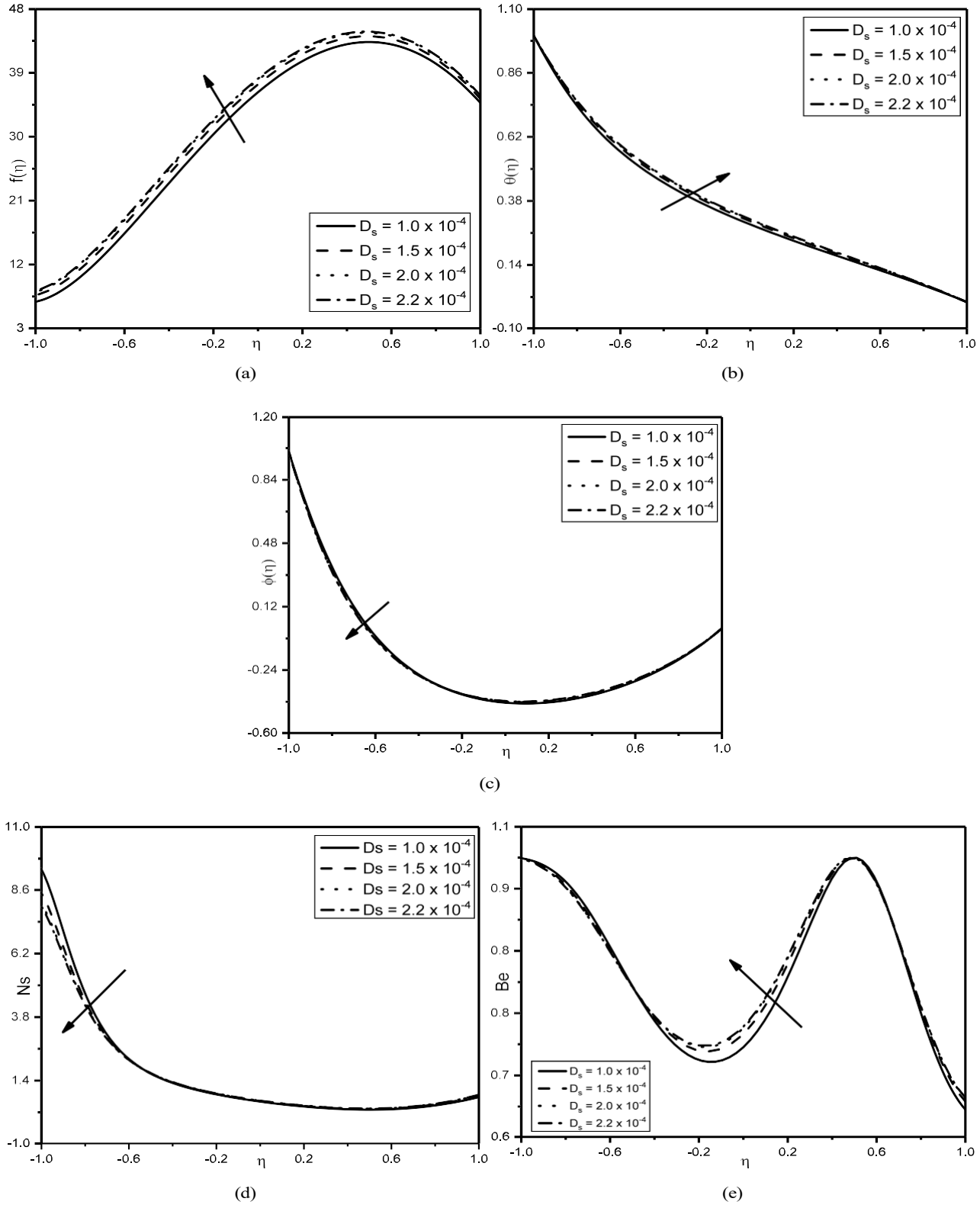

Figure 8: Influence of *Ds* on (a) *f*, (b) *θ*, (c) *φ*, (d) *Ns* and (e) *Be*

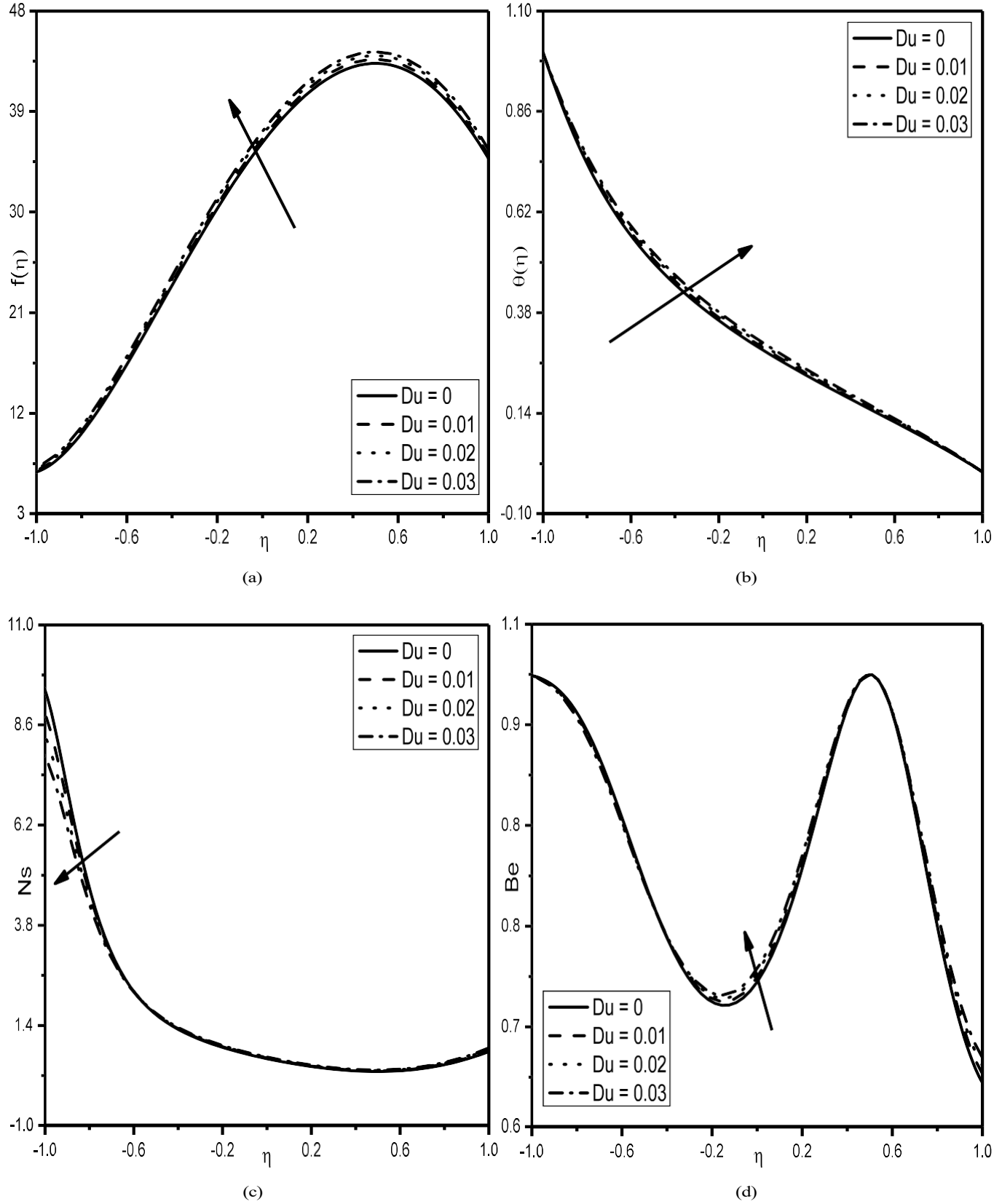

Figure 9: Influence of Du on (a) f, (b) θ, (c) N_S and (d) Be

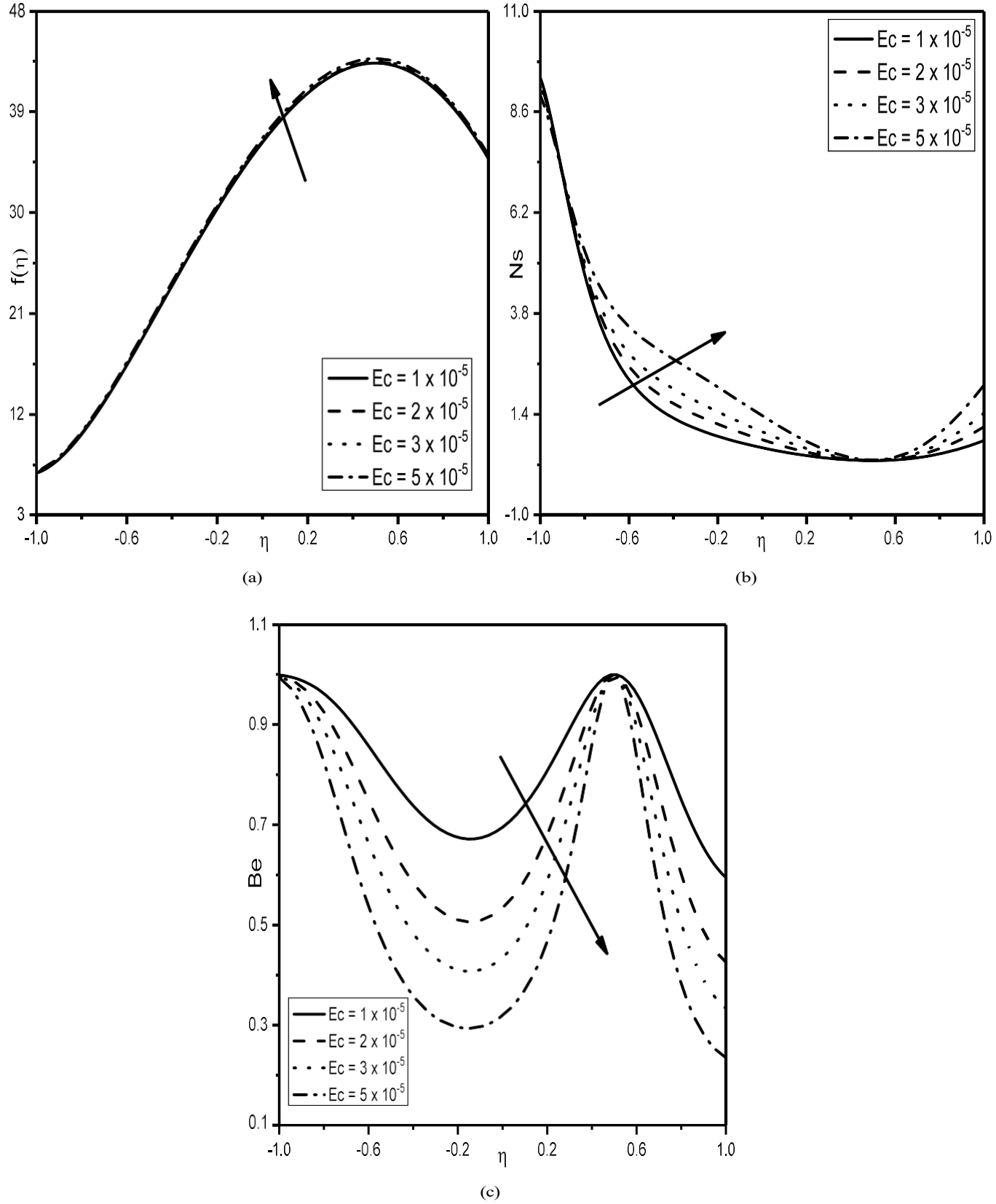

Figure 10: Influence of *Ec* on (a) *f*, (b) N_S and (c) *Be*

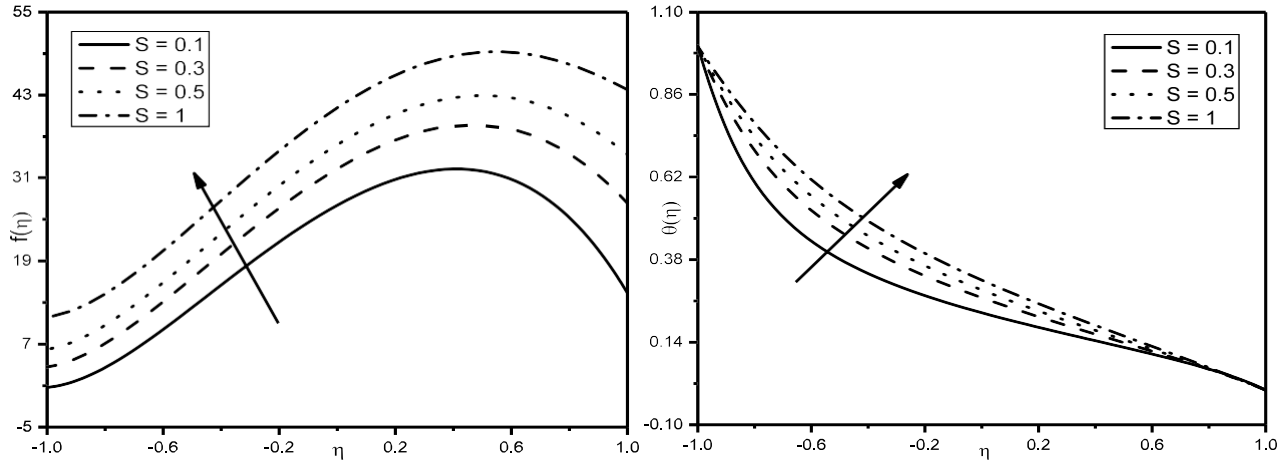

(a) (b)

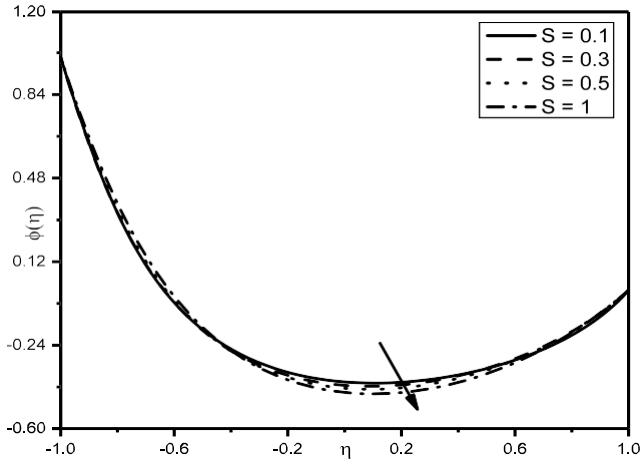

(c)

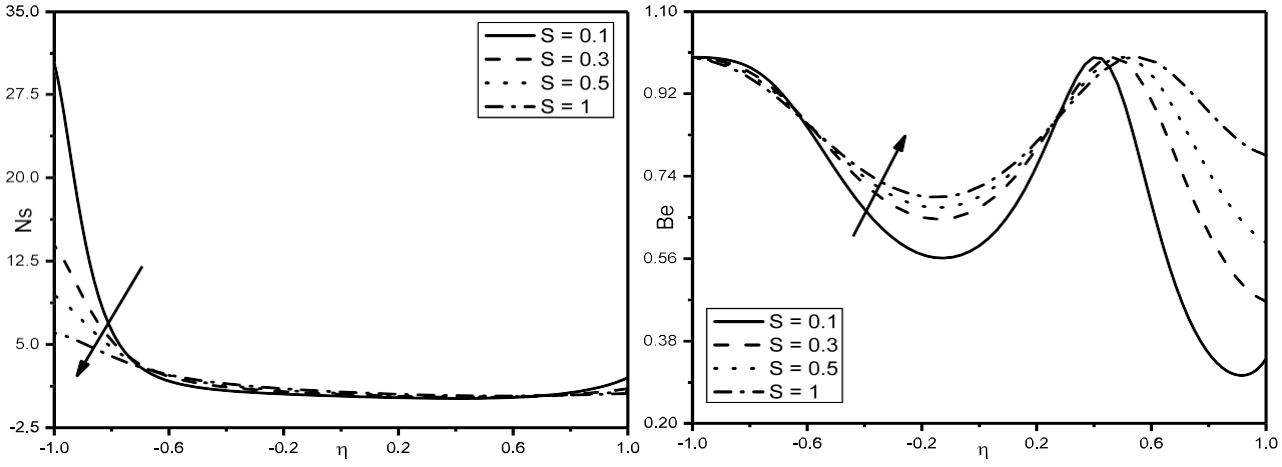

(d) (e)

Figure 11: Influence of S on (a) f, (b) θ, (c) φ, (d) N_S and (e) Be

Table 2 represents the numerical data for *Nu*, *Sh*, and C_f at lower plate due to embedded chosen parameters from this study. It can be noted, as the rising values of α and *S* Causes C_f to increase and thereby improving the quality of convective heat transfer. Whereas, with increasing values of D_h, both the skin friction coefficient and the Nusselt number increase. thus showcasing a prominent raise in quantitative data of *Nu*. Whereas, strengthening C_R, convection results in a significant decrease in *Sh* and skin friction.Meanwhile, an increase in *Du* suppresses the convective heat transfer rate by the ability of the magnetic field, Whereas, the skin friction is enhanced due to the high thermal conductivity of graphene oxide. Similarly, when strengthening *S*, elevated values observed in *Sh* and C_f.

Table 2: *Nu*, *Sh*, and C_f for varying values of embedded parameters

Re	R_{SC}	D_h	α	*Da*	*Ds*	*Du*	*Ec*	*Cr*	*S*	$-\theta'(1)$	$-\varphi'(1)$	$A_6 f''(1)$
200	5	0.1	$\pi/4$	1	0.0001	0.001	0.00002	0.1	0.5	3.027258721	8.277721288	21.41335528
300	5	0.1	$\pi/4$	1	0.0001	0.001	0.00002	0.1	0.5	3.065604245	7.91610508	12.73574828
500	5	0.1	$\pi/4$	1	0.0001	0.001	0.00002	0.1	0.5	3.081752244	7.349849513	6.177324096
700	5	0.1	$\pi/4$	1	0.0001	0.001	0.00002	0.1	0.5	3.036258277	6.942696603	3.647886024
300	-0.01	0.1	$\pi/4$	1	0.0001	0.001	0.00002	0.1	0.5	1.655487489	6.585485744	53.7635409
300	0.1	0.1	$\pi/4$	1	0.0001	0.001	0.00002	0.1	0.5	1.673852842	6.610349173	52.66494169
300	0.2	0.1	$\pi/4$	1	0.0001	0.001	0.00002	0.1	0.5	1.690823819	6.633011563	51.64681825
300	0.5	0.1	$\pi/4$	1	0.0001	0.001	0.00002	0.1	0.5	1.743340688	6.701233203	48.49977969
300	5	0.01	$\pi/4$	1	0.0001	0.001	0.00002	0.1	0.5	1.793925571	7.90793198	18.00534849
300	5	0.04	$\pi/4$	1	0.0001	0.001	0.00002	0.1	0.5	2.588915137	7.920966558	14.49797449
300	5	0.05	$\pi/4$	1	0.0001	0.001	0.00002	0.1	0.5	2.714007013	7.920622579	14.01488376
300	5	0.1	$\pi/4$	1	0.0001	0.001	0.00002	0.1	0.5	3.065604245	7.91610508	12.73574828
300	5	0.1	$\pi/6$	1	0.0001	0.001	0.00002	0.1	0.5	3.083815099	7.54269262	7.873764654
300	5	0.1	$\pi/4$	1	0.0001	0.001	0.00002	0.1	0.5	3.065604245	7.91610508	12.73574828
300	5	0.1	$\pi/3$	1	0.0001	0.001	0.00002	0.1	0.5	3.047648899	8.107665207	16.59379197
300	5	0.1	$\pi/2$	1	0.0001	0.001	0.00002	0.1	0.5	3.033356951	8.230538102	19.90182442
300	5	0.1	$\pi/4$	1	0.0001	0.001	0.00002	0.1	0.5	3.065604245	7.91610508	12.73574828
300	5	0.1	$\pi/4$	2	0.0001	0.001	0.00002	0.1	0.5	3.001079544	7.914209493	14.08007194
300	5	0.1	$\pi/4$	3	0.0001	0.001	0.00002	0.1	0.5	2.98013341	7.91317379	14.55963462
300	5	0.1	$\pi/4$	4	0.0001	0.001	0.00002	0.1	0.5	2.969757443	7.912580212	14.80583173
300	5	0.1	$\pi/4$	1	0.0001	0.001	0.00002	0.1	0.5	3.065604245	7.91610508	12.73574828
300	5	0.1	$\pi/4$	1	0.00015	0.001	0.00002	0.1	0.5	2.915115336	8.274424564	14.58987135
300	5	0.1	$\pi/4$	1	0.0002	0.001	0.00002	0.1	0.5	2.845666022	8.473491115	15.5801198
300	5	0.1	$\pi/4$	1	0.00022	0.001	0.00002	0.1	0.5	2.826960993	8.530821682	15.86806624
300	5	0.1	$\pi/4$	1	0.0001	0	0.00002	0.1	0.5	3.075332692	7.915911765	12.70084978
300	5	0.1	$\pi/4$	1	0.0001	0.01	0.00002	0.1	0.5	2.98008529	7.917751291	13.04326552
300	5	0.1	$\pi/4$	1	0.0001	0.02	0.00002	0.1	0.5	2.889011037	7.919403353	13.37218857
300	5	0.1	$\pi/4$	1	0.0001	0.03	0.00002	0.1	0.5	2.801629161	7.920895331	13.6891222
300	5	0.1	$\pi/4$	1	0.0001	0.001	0.00001	0.1	0.5	3.065604245	7.91610508	12.73574828
300	5	0.1	$\pi/4$	1	0.0001	0.001	0.00002	0.1	0.5	3.04613829	7.915602771	12.82693596
300	5	0.1	$\pi/4$	1	0.0001	0.001	0.00003	0.1	0.5	3.026782199	7.915099526	12.91777893
300	5	0.1	$\pi/4$	1	0.0001	0.001	0.00005	0.1	0.5	2.988386947	7.914090602	13.09847196
300	5	0.1	$\pi/4$	1	0.0001	0.001	0.00002	0.1	0.5	3.070750378	7.910708928	12.65244642
300	5	0.1	$\pi/4$	1	0.0001	0.001	0.00002	0.5	0.5	3.087365209	7.893707492	12.38879002
300	5	0.1	$\pi/4$	1	0.0001	0.001	0.00002	0.8	0.5	3.088934634	7.89213401	12.36429435
300	5	0.1	$\pi/4$	1	0.0001	0.001	0.00002	1	0.5	3.089458248	7.891610277	12.35613739
300	5	0.1	$\pi/4$	1	0.0001	0.001	0.00002	0.1	0.1	5.500601274	7.967641921	7.707305959
300	5	0.1	$\pi/4$	1	0.0001	0.001	0.00002	0.1	0.3	3.729154482	8.195347671	12.51942147
300	5	0.1	$\pi/4$	1	0.0001	0.001	0.00002	0.1	0.5	3.065604245	7.91610508	12.73574828
300	5	0.1	$\pi/4$	1	0.0001	0.001	0.00002	0.1	1	2.453919993	7.418472479	11.08124376

6. Conclusions

The present study investigated the slip-driven flow of graphene oxide (GO) nanofluid through an inclined channel, incorporating the combined effects of double dispersion, Chemical reaction, Dufour effect, and and viscous dissipation.

- GO nanoparticles significantly enhanced the effective thermal conductivity of the base fluid, resulting in improved heat transfer across the channel.
- Elevated velocity was recorded by strengthening slip parameter, solutal dispersion parameter, Eckert number and dufour. Hence, high the magnetic field strength promotes better velocity.
- When $Be > 0.66$, heat transfer dominates the entropy generation process, whereas variations in the governing parameters contribute only marginally through mass transfer and fluid friction effects.
- Elevated values of the Dufour and chemical reaction parameters augment skin friction and strengthen the mechanisms of convective mass transfer and conductive heat transport.
- Enhanced convective heat transfer is attained by increasing the angle of inclination, suction parameter, and slip parameter. As a result, as compared to the flow in a horizontal channel with ignored slip condition, the inclined channel achieves greater thermal performance under the influence of a magnetic field while accounting for slip velocity conditions.
- The results emphasize the need for optimal control of thermal radiation, viscous dissipation, nanoparticle concentration, and dispersion parameters to achieve enhanced heat transfer while minimizing entropy generation.
- Overall, the study provides valuable insights for designing efficient thermal management, energy storage, and cooling systems utilizing GO nanofluids in inclined channel configurations.

References

[1] Buongiorno, J.: Convective Transport in Nanofluids. J. Heat Transfer. 128, 240–250 (2006). https://doi.org/10.1115/1.2150834

[2] Abro, K.A., Abdon, A.: A computational technique for thermal analysis in coaxial cylinder of onedimensional flow of fractional Oldroyd-B nanofluid. Int. J. Ambient Energy. 43, 5357–5365 (2022). https://doi.org/10.1080/01430750.2021.1939157

[3] Akram, M., Jamshed, W., Goud, B.S., Pasha, A.A., Sajid, T., Rahman, M.M., Arshad, M., Weera, W.: Irregular heat source impact on carreau nanofluid flowing via exponential expanding cylinder: A thermal case study. Case Stud. Therm. Eng. 36, 102171 (2022). https://doi.org/10.1016/j.csite.2022.102171

[4] Shah, R.A., Ullah, H., Khan, M.S., Khan, A.: Parametric analysis of the heat transfer behavior of the nano-particle ionic-liquid flow between concentric cylinders. Adv. Mech. Eng. 13, 168781402110240 (2021). https://doi.org/10.1177/16878140211024009

[5] Javanmard, M., Salmani, H., Taheri, M.H., Askari, N., Kazemi, M.A.: Heat transfer of a radial, nanofluid

water-graphene oxide hydromagnetic flow between coaxial pipes with a variable radius ratio. Proc. Inst. Mech. Eng. Part E J. Process Mech. Eng. 235, 124–133 (2021). https://doi.org/10.1177/0954408920948194

[6] Masood, S., Farooq, M.: Influence of thermal stratification and thermal radiation on graphene oxide-Ag/H2O hybrid nanofluid. J. Therm. Anal. Calorim. 143, 1361–1370 (2021). https://doi.org/10.1007/s10973-020-10227-7

[7] Ramesh, G.K., Shehzad, S.A., Izadi, M.: Falkner–Skan flow of aqueous magnetite–graphene oxide nanoliquid driven by a wedge. Chinese J. Phys. 77, 733–746 (2022). https://doi.org/10.1016/j.cjph.2021.07.023

[8] Bhattacharyya, A., Sharma, R., Hussain, S.M., Chamkha, A.J., Mamatha, E.: A numerical and statistical approach to capture the flow characteristics of Maxwell hybrid nanofluid containing copper and graphene nanoparticles. Chinese J. Phys. 77, 1278–1290 (2022). https://doi.org/10.1016/j.cjph.2021.09.015

[9] Lavine, A. S. ”Analysis of fully developed opposing mixed convection between inclined parallel plates.” Wärme- und Stoffübertragung 23, no. 4 (1988): 249-257.

[10] Barai, Divya P., Bharat A. Bhanvase, and Shirish H. Sonawane. ”A review on graphene derivatives-based nanofluids: investigation on properties and heat transfer characteristics.” Industrial and Engineering Chemistry Research 59, no. 22 (2020): 10231-10277

[11] Azimi, Mohammadreza, Alireza Azimi, and Masoomeh Mirzaei. ”Investigation of the unsteady graphene oxide nanofluid flow between two moving plates.” Journal of Computational and Theoretical Nanoscience 11, no. 10 (2014): 2104-2108.

[12] Javanmard, M., M. H. Taheri, M. Abbasi, and S. M. Ebrahimi. ”Heat transfer analysis of hydromagnetic water–graphene oxide nanofluid flow in the channel with asymmetric forced convection on walls.” Chemical Engineering Research and Design 136 (2018): 816-824.

[13] Yadav, Pramod Kumar, and Amit Kumar Verma. ”Analysis of two non-miscible electrically conducting micropolar fluid flow through an inclined porous channel: Influence of magnetic field.” ZAMM-Journal of Applied Mathematics and Mechanics/Zeitschrift für Angewandte Mathematik und Mechanik 103, no. 1 (2023): e202200047.

[14] Ahmed, AKM Muktadir, M. D. Shamshuddin, M. Ferdows, and Mohamed R. Eid. ”Heat and mass transport through biaxial extending sheet with anisotropic slip and entropy/Bejan on the three-dimensional boundary layer hybrid nanofluid.” Proceedings of the Institution of Mechanical Engineers, Part E: Journal of Process Mechanical Engineering (2022): 09544089221147394.

[15] Srinivasacharya D, Bindu KH. Entropy generation in a micropolar fluid flow through an inclined channel with slip and convective boundary conditions. Energy. 2015 Nov 1; 91:72-83.

[16] Buongiorno, Jacopo. ”Convective transport in nanofluids.” (2006): 240-250.

[17] Gul, Taza, Malik Zaka Ullah, Abdullah Khames Alzahrani, and Iraj Sadegh Amiri. ”Thermal performance of the graphene oxide nanofluids flow in an upright channel through a permeable medium.” IEEE

Access 7 (2019): 102345-102355.

[18] K. Elsaid, M. A. Abdelkareem, H. M. Maghrabie, E. T. Sayed, T. Wilberforce, A. Baroutaji, A. G. Olabi. “Thermophysical properties of graphene-based nanofluids.” International Journal of Thermofluids 10 (2021) 100073.

[19] Al-Sankoor, K., H. Al-Gayyim, S. Al-Musaedi, Zohreh Asadi, and D. D. Ganji. ”Analytically investigating of heat transfer parameters with presence of graphene oxide nanoparticles in Williamson-magnetic fluid by AGM and HPM methods.” Case Studies in Thermal Engineering 27 (2021): 101236.

[20] Lide, David R., ed. CRC handbook of chemistry and physics. Vol. 85. CRC press, 2004.

[21] Ghadikolaei, S. S., Kh Hosseinzadeh, Mohammad Hatami, D. D. Ganji, and M. Armin. ”Investigation for squeezing flow of ethylene glycol (C2H6O2) carbon nanotubes (CNTs) in rotating stretching channel with nonlinear thermal radiation.” Journal of Molecular Liquids 263 (2018): 10-21.

[22] Chu, Yu-Ming, Kottakkaran Sooppy Nisar, Umair Khan, Hamed Daei Kasmaei, Manuel Malaver, Aurang Zaib, and Ilyas Khan. ”Mixed convection in MHD water-based molybdenum disulfide-graphene oxide hybrid nanofluid through an upright cylinder with shape factor.” Water 12, no. 6 (2020): 1723.

[23] Bejan, Adrian. ”Entropy generation minimization: The new thermodynamics of finite-size devices and finite-time processes.” Journal of Applied Physics 79, no. 3 (1996): 1191-1218.

[24] Bejan, Adrian, and J. Kestin. ”Entropy generation through heat and fluid flow.” (1983): 475-475.

[25] Paoletti, S., F. Rispoli, and E. Sciubba. ”Calculation of exergetic losses in compact heat exchanger passages.” In Asme Aes, vol. 10, no. 2, pp. 21-29. 1989.

[26] Bellman, R.E., Kalaba, R.E.: Quasilinearization and Nonlinear Boundary-Value Problems. Am. Math. Mon. 74, 1157 (1967). https://doi.org/10.2307/2313669

[27] Canuto CG, Hussaini M, Quarteroni A, Zang T. Spectral Methods - Fundamentals in Single Domains. Vol. 87. 2007.

[28] Malashetty, M.S., Umavathi, J.C., Prathap Kumar, J.: Convective magnetohydrodynamic two fluid flow and heat transfer in an inclined channel. Heat Mass Transf. 37, 259–264 (2001).

[29] Behseresht, A., Noghrehabadi, A., Ghalambaz, M.: Natural-convection heat and mass transfer from a vertical cone in porous media filled with nanofluids using the practical ranges of nanofluids thermo-physical properties. Chem. Eng. Res. Des. 92, 447–452 (2014). https://doi.org/10.1016/j.cherd.2013.08.028.

[30] A Bhattacharyya, R Kumar and G S Seth : Capturing the features of peristaltic transport of a chemically reacting couple stress fluid through an inclined symmetric channel with Dufour and Soret effects in presence of inclined magnetic field.Indian JPhys,https://doi.org/10.1007/s12648-020-01936-8

[31] Abdullahi Sammani and Hanafi Junaidu :EFFECT OF SUCTION/INJECTION ON UNSTEADY MHD NATURAL CONVECTION FLOW OF HEAT MASS TRANSFER IN

POROUS CHANNEL IN THE
PRESENCE OF SORET TERM,Advanced Journal of Science, Technology and Engineering, DOI URL: https://doi.org/10.52589/AJSTE-3TYZFHWH

[32] Salisu Saleh, Sheriff Abdulazeez and Omokhuale Emmanuel : MAGNETOHYDRODYNAMIC (MHD) CON- VECTIVE FLOW IN A POROUS MEDIUM WITH SUCTION/ INJECTION AND DUFOUR EFFECTS
,Journal of Basic Physical Research ISSN: 2141-8403 Prints, 2141-8411 Online,Vol.12, No.1 pp. 21- 29 March., 2024

[33] Achogo, Wisdom Hezekiah, Isobeye George, Nwagor Peters : Heat Generation and Dufour Influences on MHD Convective Flow through an Inclined Channel , International Journal of Research and Scientific Innovation (IJRSI) —Volume VIII, Issue V, May 2021—ISSN 2321-2705

[34] Utpal Jyoti Dasa and Sonam Dorjeeb : Unsteady MHD oscillatory visco-elastic fluid flow through an inclined channel in presence of chemical reaction with Soret and Dufour effects ,Indian Journal of Pure and Applied Physics Vol. 58, September 2020, pp. 691-697

[35] Achogo, Wisdom Hezekiah, Adikabu, Ile Nwachukwu, Awortu, Ibifaa, Eleonu, Blessing Chikaodi : Soret Effect on MHD Free Convection through a Porous Inclined Channel in the Presence of Thermal Radiation
,International Journal of Research and Innovation in Applied Science (IJRIAS) — Volume V, Issue VII, July 2020—ISSN 2454-6194

[36] Odelu Ojjela, Adigoppula Raju, N. Naresh Kumar : INFLUENCE OF INDUCED MAGNETIC FIELD AND RADIATION ON FREE CONVECTIVE JEFFREY FLUID FLOW BETWEEN TWO PARALLEL POROUS
PLATES WITH SORET AND DUFOUR EFFECTS ,Journal of Mechanics Vol 35, No 5, October 2019 ,DOI
: 10.1017/jmech.2018.68

[37] Khuram Rafique , Muhammad Imran Anwar, Masnita Misiran , Ilyas Khan , Asiful H. Seikh , El-Sayed M. Sherif, and Kottakkaran Sooppy Nisar : Brownian Motion and Thermophoretic Diffusion Effects on Micropolar Type Nanofluid Flow with Soret and Dufour Impacts over an Inclined Sheet:Keller-Box Simulations ,Energies 2019, 12, 4191; doi:10.3390/en12214191

[38] Yusuf A, Alyesimi Y M , Jiya M, Okedayo G T, : Analysis of Couette Flow of a Nanofluid in an Inclined Channel with Soret and Dufour Effects , Scientific and Academic Publishing, American Nournal of Computational and Applied Mathematics, doi: 10.5923/j.ajcam.20160602.05

[39] K. Vijaykumar and E. Keshava Reddy : Joule Heating and Radiation Absorption Effects on MHD Convective and Chemically Reactive Flow Past an Inclined Porous Plate ,International Journal of Research and Scientific Innovation (IJRSI) — Volume IV, Issue VIII, August 2017 — ISSN 2321–2705

[40] S. Ravikumar, J. Suresh Goud , P. Srilatha, R. Sivaiah, SK. Abzal : Joule Heating and Thermal Radiation

Effects on MHD Peristaltic Couple Stress Hemodynamic Fluid Model through an Inclined Channel with Chemical Reaction , International Journal of Pure and Applied Mathematics, Volume 120 No. 5 2018, 967-981,ISSN: 1314-3395, url:http://www.acadpubl.eu/hub/

[41] Akinbowale T. Akinshilo : Mixed convective heat transfer analysis of MHD fluid flowing through an electrically conducting and non-conducting walls of a vertical micro-channel considering radiation effect ,Applied Thermal Engineering,https://doi.org/10.1016/j.applthermaleng.2019.04.100

[42] Achogo, Wisdom Hezekiah , Okereke, Ifeoma Chikamma , Ofomata, Amarachukwu I, Amadi Onyebuchi Fe- licia : Magnetohydrodynamic Convective Periodic Flow through a Porous Medium in an Inclined Channel with Thermal Radiation and Chemical Reaction, International Journal of Innovative Science and Research Technology,ISSN No:-2456-2165,Volume 5, Issue 1, January – 2020

[43] S. Suresh Kumar Raju : Dynamical dissipative and radiative fow of comparative an irreversibility analysis of micropolar and hybrid nanofuid over a Joule heating inclined channel ,Scientifc Reports (2023) 13:5356 https://doi.org/10.1038/s41598-023-31920-1

[44] A. M. Bouaziz,S. Hanini: DOUBLE DISPERSION FOR DOUBLE DIFFUSIVE BOUNDARY LAYER IN NON-DARCY SATURATED POROUS MEDIUM FILLED BY A NANOFLUID ,Journal of Mechanics,DOI : 10.1017/jmech.2016.18

[45] A S Sabu, Alphonsa Mathew , Neethu T S , Anil George K : Statistical Analysis of MHD Convective Ferro-nanofluid Flow through an Inclined Channel with Hall Current, Heat Source and Soret Effect ,Thermal Science and Engineering Progress (2020), doi: https://doi.org/10.1016/j.tsep.2020.100816

[46] Shafqat Hussain : Finite Element Solution for MHD Flow of Nanofluids with Heat and Mass Transfer through a Porous Media with Thermal Radiation, Viscous Dissipation and Chemical Reaction Effects , Advances in Applied Mathematics and Mechanics, Adv. Appl. Math. Mech., Vol. 9, No. 4, pp. 904-923,DOI: 10.4208/aamm.2014.m793,August 2017

[47] Basant K. Jha and Taiwo S. Yusuf : Entropy generation in an inclined porous channel with suction/injection , Nonlinear Engineering 2020; 9: 103–110,https://doi.org/10.1515/nleng-2018-0116

[48] Humnekar, N., & Srinivasacharya, D. (2024). Influence of variable viscosity and double diffusion on the convective stability of nanofluid flow in an inclined porous channel. Applied Mathematics and Mechanics (English Edition), 45(3), 563–580. https://doi.org/10.1007/s10483-024-3096-6

[49] Sarma, S., Reddy, G. J., & Rao, M. V. S. (2022). Dufour effect on unsteady MHD flow past a vertical plate in a porous medium. Scientific Reports, 12, 17458. https://doi.org/10.1038/s41598-022-21945-3

[50] Vinod, Y. (2024). Dufour and Soret effects on double-diffusive Casson fluid flow with internal heat source. Applied Mathematics and Mechanics (English Edition), 45(7), 1085–1102. https://doi.org/10.1007/s10483-024-3141-5

[51] Eid, M. R. (2023). Mathematical analysis of energy transfer in micropolar fluid flow with Dufour effect and viscous dissipation. Computers & Fluids, 252, 105707. https://doi.org/10.1016/j.compfluid.2023.105707

[52] Dev, K. (2024). Double-diffusive convection in a porous layer subjected to an inclined thermal gradient. International Journal of Heat and Mass Transfer, 214, 124567. https://doi.org/10.1016/j.ijheatmasstransfer.2023.124567

[53] Manigandan, C., Senthamilselvi, S., Bhavani, S., & Rekha, V. (2025). Chemical reaction and radiation effects on Dufour and heat source influences in Casson fluid flow over an inclined oscillating plate. Journal of Information Systems Engineering and Management, 10(32s), 1–12.

[54] Ahamedsheriff, S., Rajaram, V., Mani, G., & co-authors (2025). Impacts of Soret and Dufour effects on micropolar fluid flow past a stretching sheet in a porous medium. Scientific Reports, 15, 33059. https://doi.org/10.1038/s41598-025-18302-5

[55] Dawood, A. S., Kroush, F. A., & Abumandour, R. M. (2024). Effect of slip boundary conditions on unsteady pulsatile nanofluid flow through a sinusoidal channel: An analytical study. Boundary Value Problems, 2024, Article 62. https://doi.org/10.1186/s13661-024-01862-2

[56] Sinha, A. (2025). Impact of thermal radiation, Dufour effect, and chemical reaction on oscillatory MHD flow through porous media. International Journal for Multidisciplinary Research, 7(4), 1–10.